Constitutive Model of the Multiaxial Strength of Concrete at High Temperature

K.-Ch. Thienel, F. S. Rostásy, U. Diederichs
Institut für Baustoffe, (Massivbau und Brandschutz) Braunschweig, FRG

1. INTRODUCTION

In order to improve the safety analysis of the HTR reliable high temperature test data concerning strength and deformation of the concrete and relevant constitutive material laws applicable in FEM-analysis are needed. This holds especially for the concrete of the PCRV, for which hypothetical accident temperatures up to 1000 °C have to be considered. Extensive experimental investigations on basalt concrete have been pursued by Hochtemperatur-Reaktorbau GmbH within the HTR 500 developmental work. The investigations were carried out at the Institut für Baustoffe, Massivbau und Brandschutz, Technical University, Braunschweig, and at other institutes. The requirements of the material characteristics are given in the report of Weber et al. (1985) and Schneider et al. (1984). Based on the extensive test results on PCRV-concrete and and on additional tests carried out for this report, a first parameter fit for the 5-Parameter-Model of Willam-Warnke for the temperature range of 20 °C to 600 °C will be described.

2. EXPERIMENTAL WORK

The data used for the parameter fit were gained from tests which were performed with the basalt concrete. All specimens were demoulded one day after casting and subsequently stored under water for more than 90 d until testing.

One set of data was taken from uniaxial residual tension tests performed with a concrete similar to the HRB-basalt concrete on cylindrical specimens (Ø 80 mm, h = 150 mm). This data can be regarded as lower limit of the tensile strength (Diederichs, 1983).

Uniaxial compressive strength data at temperatur levels of 450 °C, 500 °C and 600 °C were taken from tests on cylindrical specimens (Ø 80 mm, h = 240 mm) (Diederichs, 1989).

Biaxial compression tests were carried out in a special high temperature biaxial test set-up. In these experiments disc-shaped specimens (200 mm x 200 mm x 50 mm) were used. The specimens were saw-cut from cubes (200 mm x 200 mm x 200 mm). Loading was performed with "loading brushes" to provide a defined, homogeneous stress state (Ehm, 1986). The biaxial specimens were loaded with a given stress ratio (σ_2/σ_1 = 0.0; 0.2; 0.4; 0.66; 1.0). Test temperatures were: 20 °C, 70 °C, 120 °C, 200 °C, 300 °C, 450 °C, 500 °C and 600 °C.

In the uniaxial compression tests the specimens were loaded at ambient temperature (20 °C) with 15 N/mm^2 in their first axis and in the biaxial tests corresponding to the stress ratio with a lower load in the second axis. All specimens were heated up unsealed at a heating rate of 5 K/h up to 70 °C and 20 K/h above 70 °C. The specimens for compressive tests were loaded up to rupture after a holding period of one hour.

3. CONSTITUTIVE MODEL

The parameters of the Willam-Warnke-Model have to be replaced by approximated temperature dependent functions to describe the multiaxial failure surface at high temperature. This failure surface is defined in principal stress space by a homogeneous expansion in the "average" stress components σ_a, τ_a and the angle of similarity θ.

$$f(\sigma,T) = f(\sigma_a,\tau_a,\theta,T) = \frac{1}{r(\sigma_a,\theta)}\,\frac{\tau_a}{f_{cu}} - 1 = 0$$

with: σ_a : average normal stress

τ_a : average shear stress

f_{cu}: uniaxial compressive strength

T : temperature in °C

and

$$r(\sigma_a,\theta) = \frac{2r_2(r_2^2-r_1^2)\cos\theta+r_2(2r_1-r_2)[4(r_2^2-r_1^2)\cos^2\theta+5r_1^2-4r_1r_2]^{\frac{1}{2}}}{4(r_2^2-r_1^2)\cos^2\theta+(r_2-2r_1)^2}$$

with: r_1: position vector at $\theta = 0°$

r_2: position vector at $\theta = 60°$

The vectors are functions of the average stress σ_a

$$r_1 = a_0 + a_1 \frac{\sigma_a}{f_{cu}} + a_2 \frac{\sigma_a^2}{f_{cu}^2}$$

$$r_2 = b_0 + b_1 \frac{\sigma_a}{f_{cu}} + b_2 \frac{\sigma_a^2}{f_{cu}^2}$$

The six constants a_0, a_1, a_2, b_0, b_1, b_2 are substituted by five parameters. These parameters are identified by temperature dependent experimental data such as the uniaxial tension strength f_t, the uniaxial compression strength f_{cu} and the biaxial compression strength f_{cb} ($\sigma_1 = \sigma_2$). Normalisation leads to the strength ratios

$$\alpha_u(T) = \frac{f_{cb}(T)}{f_{cu}(T)} ; \qquad \alpha_z(T) = \frac{f_t(T)}{f_{cu}(T)}$$

In addition to these date three strength values in high compression regime are used

$$\xi(T) = - \frac{\sigma_{at}(T)}{f_{cu}(T)} ; \ \rho_1(T) = \frac{\tau_{a1t}(T)}{f_{cu}(T)} \text{ at } \theta = 0° ; \ \rho_2(T) = \frac{\tau_{a2t}(T)}{f_{cu}(T)} \text{ at } \theta = 60°$$

with:

σ_{at} : mean normal stress test data

τ_{a1t} : mean shear stress test data at $\theta = 0°$

τ_{a2t} : mean shear stress test data at $\theta = 60°$

4. RESULTS AND DISCUSSION

The parameter α_u and α_z are directly derived from uniaxial and biaxial tests at different temperature without approximation by functions. To compute the parameters ξ, ρ_1 and ρ_2 triaxial test data are only available at ambient temperature. Thus, these parameters have to be determined for each temperature level by variation in order to minimize difference between biaxial test data and the calculated failure surface. The resulting parameters were approximated by temperature dependent polynominals:

$$\xi = 1.42\cdot10^{-6}\cdot T^2 + 9.11\cdot10^{-4}\cdot T + 0.961$$

$$\rho_1 = 3.13\cdot10^{-9}\cdot T^3 - 1.48\cdot10^{-7}\cdot T^2 - 5.31\cdot10^{-4}\cdot T + 0.560$$

$$\rho_2 = 5.57\cdot10^{-9}\cdot T^3 + 5\cdot10^{-6}\cdot T^2 - 0.00166\cdot T + 0.602$$

The calculated biaxial failure surfaces for ambient temperature, and 70 °C and 120 °C are shown in Fig. 1. There is an affine connection between these three failure envelopes. The results correspond to other results at ambient temperature (Kupfer, 1973). Another set of biaxial surfaces for 200 °C, 300 °C, 450 °C and 500 °C is shown in Fig. 2. The difference between these envelopes and the shape of the curve at 600 °C is results from the phase modification occuring in quartzitic coarse aggregates.

5. CONCLUSIONS

With the derived constitutive model the ultimate load analysis of a PCRV when subjected to very high temperature and high mechanical stresses becomes possible. Especially, the compression-compression region of the biaxial failure envelopes precisely describes the high temperature test results. For the description of the spatial failure surface a series of assumptions had to be made because of lack of data. For such regimes, further experimental research is necessary.

6. REFERENCES

Diederichs, U. und Ehm, C. (1968): Mechanisches Verhalten von HTR-Beton, Teil 5: Biaxiale Druckversuche. Bericht über eine im Auftrag der Hochtemperatur-Reaktorbau GmbH, Mannheim, durchgeführte Untersuchung. Institut für Baustoffe, Massivbau und Brandschutz der Technischen Universität Braunschweig. Braunschweig, Juni 1986.

Ehm, C. (1986): Versuche zur Festigkeit und Verformung von Beton unter zweiaxialer Beanspruchung und hohen Temperaturen (Dissertation). Heft 71 der Schriftenreihe des Instituts für Baustoffe, Massivbau und Brandschutz der Technischen Universität Braunschweig, Braunschweig 1986.

Diederichs, U. (1983): Hochtemperaturverhalten von Festbeton, Arbeitsbericht 1981 - 1983, Teil 2, B3-86, des Sonderforschungsbereichs 148 "Brandverhalten von Bauteilen", TU Braunschweig, Mai 1983.

Kupfer, H. (1973): Das Verhalten des Betons unter mehrachsiger Kurzzeitbelastung unter besonderer Berücksichtigung der zweiachsigen Beanspruchung. Heft 229 des DAfStb, Berlin 1973.

Schneider, U.; Diederichs U. und Weber, A. (1984): Behaviour of HTR-concrete at elevated temperatures - State-of-the-art. Specialists Meeting on Design, Criteria and Experience with prestressed Reactor Pressure Vessels for Gas Cooled Reactors, International Atomic Energy Agency, Vienna, held in Lausanne, Switzerland, 1984.

Weber, A. und Diederichs, U. (1985): Effects of long-term thermal exposure on the behaviour of HTR-concrete Proceedings of the 8th International Conference on "Structural Mechanics in Reactor Technology", Brussels (Belgium), 19. - 23. August 1985, Volume H, Paper H 5/3.

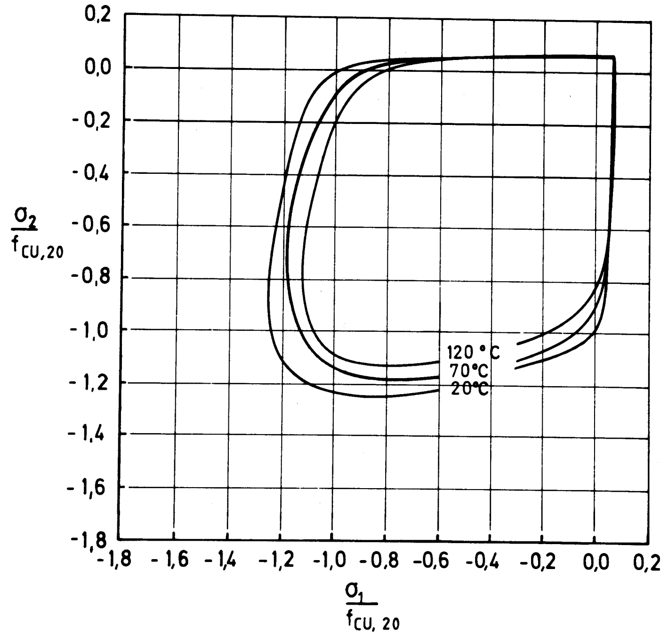

Figure 1 : Computed failure surface for 20 °C, 70 °C and 120 °C

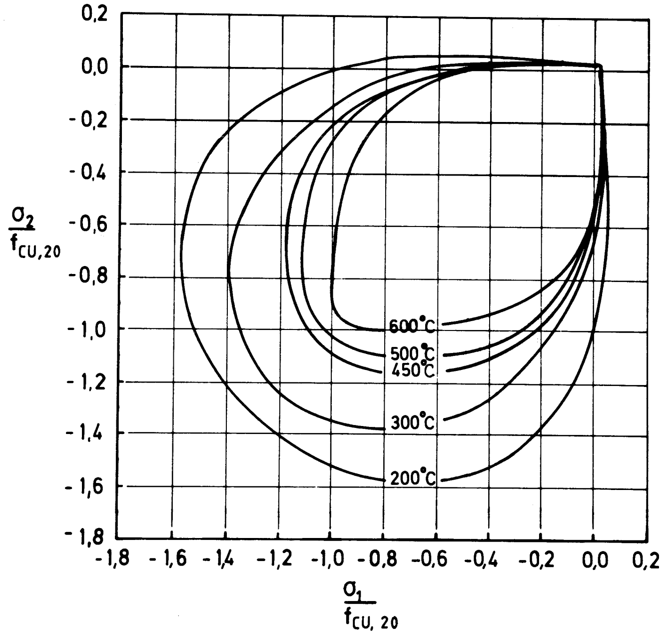

Figure 2 : Computed failure surface for 200 °C, 300 °C, 450 °C, 500 °C and 600 °C